# Refractometric sensor based on all-fiber coaxial Michelson and Mach-Zehnder interferometers for ethanol detection in fuel



2011 J. Phys.: Conf. Ser. 274 012020

(http://iopscience.iop.org/1742-6596/274/1/012020)

Journal of Physics: Conference Series **274** (2011) 012020 doi:10.1088/1742-6596/274/1/012020

# Refractometric sensor based on all-fiber coaxial Michelson and Mach-Zehnder interferometers for ethanol detection in fuel.

**L. Mosquera[1,2], Jonas H. Osório[1], Juliano G. Hayashi[1], Cristiano M.B. Cordeiro[1]**

*[1]Instituto de Fisica "Gleb Wataghin", UNICAMP, Campinas – São Paulo – Brasil; [2]Facultad de Ingeniería Civil, Universidad Nacional de Ingeniería, Avenida Túpac Amaru 210, El Rímac, PE-Lima 025, Perú;*

*Email-: lmosquera@uni.edu.pe*

**Abstract**. A refractometric sensor based on mechanically induced interferometers formed with long period gratings is reported. It is also shown two different setups based on a Michelson and Mach-Zender interferometer and its application to measure ethanol concentration in gasoline.

***Index Terms:*** *mechanically-induced long-period fiber gratings; fiber-optic refractive index sensor, chemical sensor.*

## 1. Introduction

A long-period fiber grating (LPG) is a periodic perturbation of fiber refractive index, which can couple the core mode to co-propagating cladding modes at different wavelengths. This grating transmission spectrum presents attenuation bands, which occur due to the coupling between core and cladding modes. Such attenuation band wavelength location is sensitive to temperature, surrounding medium refractive index and bends in fiber [1-4]. Literature reports a great variability in LPG fabrication techniques in recent years in order to achieve the necessary changes in the index profile. Techniques based on the use of $CO_2$ and femto-second lasers are reported as well as mechanical methods [5-7].

The mechanically-induced long-period fiber gratings (MLPGs) are attractive due to their simplicity and inexpensiveness [8, 9]. MLPGs can be built up on any kind of single mode fibers or even on holey fibers, so that their attenuation loss can be controlled in real time what makes them very promising for spectral filtering, gain equalization and others applications.

Optical fiber sensors are ideal for the detection of substances dissolved in gasoline due to its passive electrical operation [15]. In this paper, an interferometric method was used to detect percentages of ethanol dissolved in gasoline. The interferometric method was used since the MLPGs resonances are usually very wide. We increase la measurement resolution employing two experimental setups – a Michelson interferometer and a Mach-Zehnder interferometer– the sensors were performed and tested. In both cases the sensors detected changes in a gasoline-ethanol mixture refractive index – obtained by varying the ethanol concentration in mixture. The obtained results showed a sensitivity of

27 pm/% ethanol for the Michelson interferometer configuration and of 25 pm/% ethanol for Mach-Zehnder configuration.

Mechanic fatigue has not been investigated systematically in this work, but we have observed that the pressure can be applied to the same fiber many times without observing changes in the transmission spectra of the induced grating. it agrees with what is reported in the references [8,9]. Thus, with the appropriate design and material to manufacture the device, this can be applied in work site.

## 2. MLPGs

we report gratings induced on a commercial single mode fiber. Figure 1 show the experimental setup used to induce the MLPGs that consist of applying pressure onto the fiber using a corrugated board. The effect of this pressure is to make fiber refractive index to be modulated, producing the grating. Thereby, by launching a broadband light into one end of the fiber, grating transmission spectrum can be visualized with an optical spectrum analyzer (OSA Ando AQ-6315).

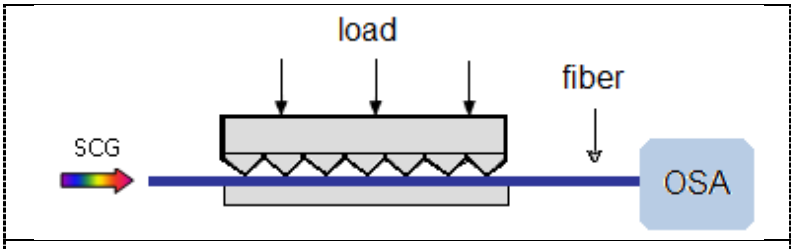


**Figure 1.** Schematic of the experimental setup to produce MLPGs by mechanical stress. SCG: supercontinuum generation in photonic crystal fibers.

Figure 2 presents the transmission spectrum for a MLPG induced with the described technique. The spectrum shown above in Figure 2 has dips at wavelengths 1403 nm, 1472 nm and 1549 nm, corresponding to the resonances with the different cladding modes. These resonances between the propagating core mode and the forward-propagating cladding mode are observed at wavelength $\lambda_n$ that satisfies Eq. (1) [1, 2].

$$\lambda_n = (n_{co}^{01} - n_{clad}^{0n})\Lambda \tag{1}$$

Where $n_{co}^{01}$ is the effective refractive index of the propagating core mode, $n_{clad}^{0n}$ is the effective refractive index of the nth cladding mode and $\Lambda$ is the LPGs period.

Figure 2 also shows that for the situation when the pressure applied on the fiber is increased, the transmission loss is increased to near -15 dB. The observed variation in dips depth is described by Eq (2) [1, 2].

$$\frac{P_{clad}^{n}(L)}{P_{01}(0)} = \frac{\sin^2[k_n L\sqrt{1+\left(\frac{\delta}{k_n}\right)^2}]}{1+(\frac{\delta}{k_n})^2} \tag{2}$$

Where, $P_{clad}^{n}(L)$ is the power coupled into the nth-cladding mode, $P_{01}(0)$ is the initial power contained in the guided $LP_{01}$ mode, L is the MLPGs length, $k_n$ is the coupling coefficient for the nth cladding mode $LP_{0n}$ and $\delta$ is the detuning parameter which can be calculated by Eq. (3).

$$\delta = \frac{1}{2}\left(\beta_{01} - \beta_{clad}^{(n)} - \frac{2\pi}{\Lambda}\right) \tag{3}$$

Where $\beta_{01}$ is the core mode propagation constant and $\beta_{clad}^{(n)}$ is cladding mode propagation constant.

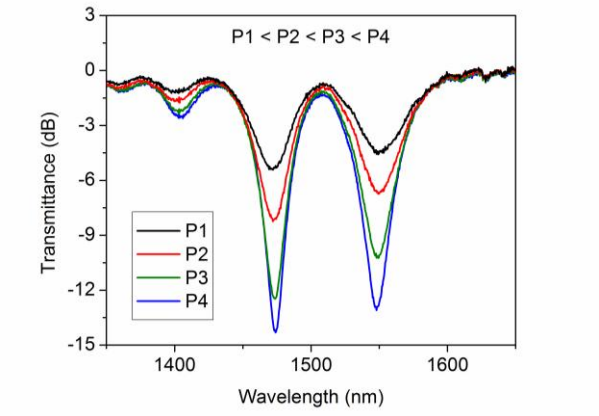


**Figure 2.** Transmission spectrum for MLPG (500 µm pitch and 20 mm long) induced in a single mode fiber as a function of the applied pressure ($P_n$).

## 3. Michelson Interferometer

The MLPG-based Michelson interferometer was built by coating the end face of the fiber in which the MLPG is made up with a golden mirror in a "folded" interferometer configuration. The schematic diagram for this sensor is shown in Figure 3. This setup is termed a self-interfering long-period grating [10, 11] which is analogous to a Michelson interferometer.

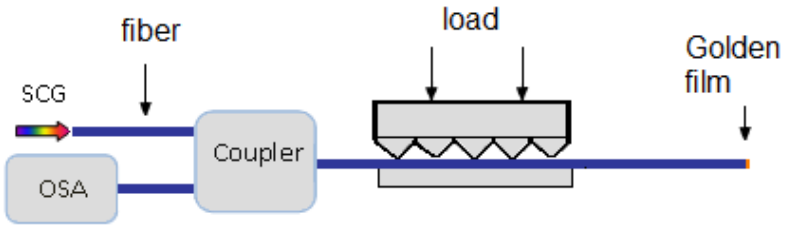


**Figure 3.** Schematic diagram of the MLPG-based Michelson Interferometer sensor.

In this configuration, the MLPG acts as a beam splitter. Since coupling the core to cladding mode, it generates the two arms of the interferometer. As a golden film is placed at the end of the fiber, reflection of both modes is observed. In the waves way back, the grating recouples the cladding mode to the core mode and an interference pattern can be observed in the reflection spectrum. Figure 4 shows the interferometers response generated in a configuration employing a MLPG 20 mm long and with a period of 500 µm.

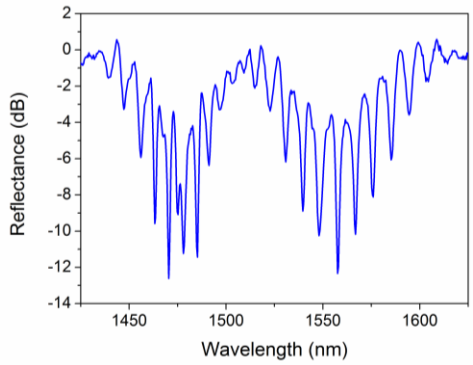


**Figure 4.** Interference pattern generated from MLPG-Michelson interferometer (MLPG 20 mm long and with 500µm pitch).

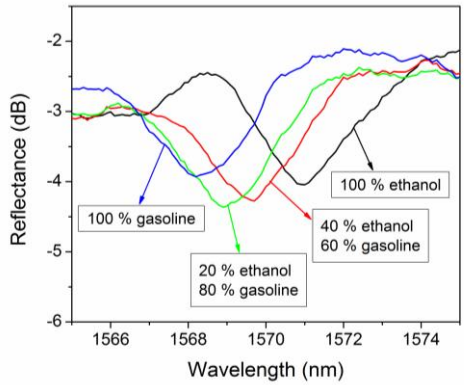


**Figure 5.** Spectral shift of an interferometric fringe from MLPG-Michelson interferometer sensor as a function of ethanol concentration in gasoline. MLPG: $\Lambda$=500µm; L = 20mm; $L_{cav}$= 73 mm.

In order to obtain a good response for the interferometer (interference fringes with good visibility), the pressure on the fiber is gradually increased. Also varying the length of fiber between the grating and the mirror (denominated $L_{CAV}$), the number of fringes observed at the interferometers spectrum varies. The increase in the number of fringes makes the fringe spectral width to be decreased, improving sensors resolution.

Thus, as the MLPGs dips localization is dependent on the external refractive index (since the gratings resonance wavelength depends on the cladding modes effective index), it is possible to perform a measurement of the external index changes by using the interferometer configuration. Ethanol concentration in gasoline was chosen to be the analyzed parameter. Therefore, the length of fiber behind the grating was immersed in a group of solutions with different percentages of ethanol in gasoline. As each solution has a different value for its refractive index, interferometers response is altered by changing the liquid in contact with the fiber. Ergo, a shift in the interference fringe position when the external environment refractive index is changed is expected. Figure 5 shows sensors response of an individual fringe in function of ethanol concentration in gasoline. Figure 6 presents a plot that relates the spectral shift to ethanol concentration in gasoline. Sensors sensitivity was 27 pm/% ethanol dissolved in gasoline.

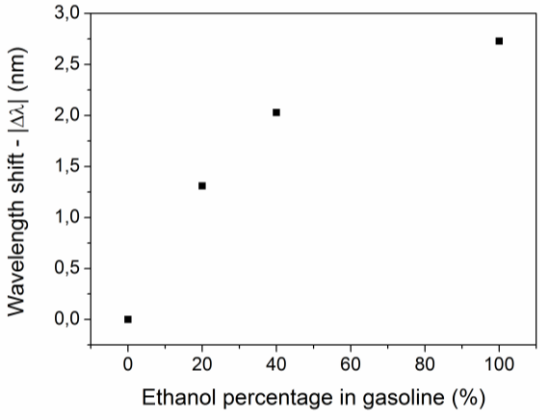


**Figure 6.** MLPG-Michelson interferometer sensitivity to changes in the percentage of ethanol dissolved in pure gasoline.

## 4. Mach-Zehnder Interferometer

A Mach-Zehnder interferometer based on a pair of MLPGs with period Λ = 500 μm and length L = 20 mm was also built. The physical phenomenon which occurs for this configuration is essentially the same that happens for the first interferometer configuration (Michelson interferometer). However, for the Mach-Zehnder configuration, the golden mirror is substituted by a second MLPG which will recouple the cladding mode to the core mode. Figure 7 presents a diagram for this setup.

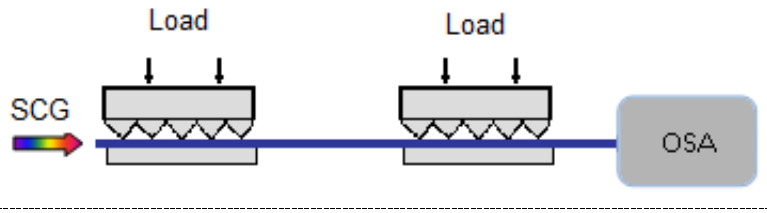


**Figure 7.** Schematic diagram of the MLPG-based sensor Mach-Zehnder Interferometer.

The procedure for producing the interferometer consists on, *a priori*, recording the first grating and, afterwards, on implementing the second grating by gradually increasing the pressure on the fiber. Thus, when a good spectrum is obtained, the pressure increase exerted is stopped by the second grating. Figure 8 shows the transmission spectrum for the first MLPG and for the interferometer response.

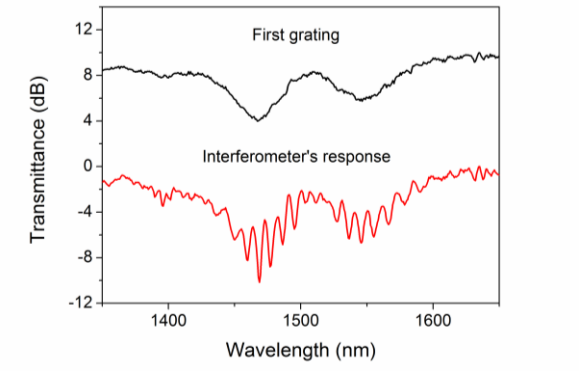


**Figure 8.** The measured transmission spectrum for the first grating (20 mm long and 500 μm pitch) and for the MLPG-Mach-Zehnder interferometer response (Distance between the gratings: $2L_{CAV}$ = 45 mm).

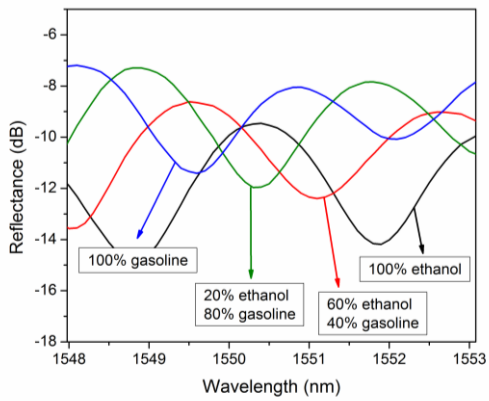


**Figure 9.** Spectral shift of an interferometric fringe from the MLPG-Mach-Zehnder interferometer spectrum as a function of ethanol percentage in gasoline (gratings 20 mm long and with 500 μm period; 2 $L_{CAV}$ = 73 mm).

This device was also used to detect percentages of ethanol dissolved in pure gasoline. Figure 9 shows the spectral shift for one of the fringes from interference pattern when different percentages of ethanol were dissolved in the gasoline. Figure 10 presents a graph for the wavelength shift in function of the ethanol percentage in gasoline. This device sensibility was 25 pm /% ethanol dissolved in gasoline.

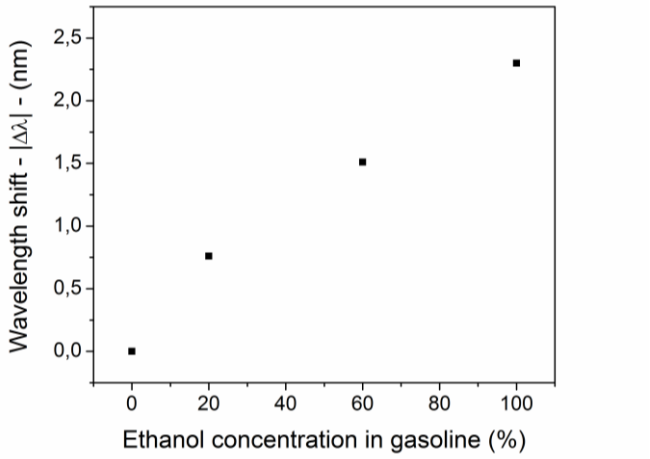


**Figure 10.** MLPG-Mach-Zehnder interferometer sensitivity to changes in the percentage of ethanol dissolved in pure gasoline.

## 5. Conclusions

In this paper, the development of mechanically induced long-period gratings (MLPGs) and their application as surrounding medium refractive index sensors were reported. Gratings with dips 17 dB deep were achieved.

Two interferometers could be built: a Michelson interferometer, based on the use of a unique MLPG and a mirror at the end of the fiber; and a Mach-Zehnder interferometer constituted by two serial MLPGs. Both devices were applied as sensors in order to detect dissolved ethanol percentages in gasoline. Interferometers resolution, determined by the dips width in MLPGs resonance band as well as by the length of fiber behind the grating for the case of Michelson configuration and by the distance between the gratings for the case of Mach-Zehnder configuration, was enough to detect changes in ethanol percentages in gasoline. Interference fringes visibility was easily optimized by apparatus versatility in adjusting the coupling between core and cladding modes. The achieved sensibility was 27 pm /% of ethanol in gasoline (Michelson interferometer) and 25 pm /% of ethanol in gasoline (Mach-Zehnder interferometer).

## 6. References

[1] Ashish M V, Lemaire P J, Judkins J B, Bhatia V, Turan E and Sipe J E 1996 *J. Lightwave Tech.* **14** Nº 1

[2] James S W and Tatam RP 2003 *Meas. Sci. Technol.* **14** R49-61

[3] Chomát M, Berková D, Matejec V, Kasík I, Kanka J, Slavík R, Jancárek A and Bittner P 2006 *Mater. Sci. Eng.* C **26** 457-61

[4] Petrovic J S, Dobb H, Mezentsev V K, Kyriacos K, Webb D J and Bennion I 2007 *J. Lightwave Tech.* **25** Nº 5

[5] Chan H M, Fares A, Tomov I V and Lee H P 2008 *IEEE Photon. Technol. Lett.* **20** Nº 8

[6] Dürr F, Rego G, Marques P V S, Semjonov S L, Dianov E M, Limberger H G and Salathé R P 2005 *J. Lightwave Tech.* **23** Nº 11

[7] Smietana M, Bock W J and Mikulic P 2010 *Meas. Sci. Technol.* **21**

[8] Savin S, Digonnet M J F, Kino G S and Shaw H J 2000 Optic. Lett. **25** Nº 10

[9] Xiaojun Z, Chen C, Zhang Z, Qin Z and Liu Y 2009 *14th OptoElectronics and Communications Conf. OECC* art. Nº 5218070

[10] Swart P L 2004 *Meas. Sci. Technol.* **15** 1576-80

[11] Barrios P, Sáez R D, Rodríguez A, Cruz J L, Díez A and Andrés M V 2009 J. Sensors ID 815409

[12] Liu Y, Williams J A R, Zhang L and Bennion I 1999 *Opt. Commun.* **164** 27-31

[13] Wei T, Lan X and Xiao H 2009 *IEEE Photon. Technol. Lett.* **21** Nº 10 669-71

[14] Young-Geun H, Lee B H, Won-Taek H, Paek U C and Chung Y 2001 *Meas. Sci. Technol.* **12** 778-81

[15] Falate R, Kamikawachi R C, Fabris J L, Müller M, Kalinowski H J, Ferri F A S, and Czelusniak L K 2003 *Proc. Microwave and Optoelectronics Conference (20-23 Sept 2003)* vol. 2 pp 907-10